Observation of reduction of radiation-pressure-induced rotational anti-spring effect on a 23 mg mirror in a Fabry–Perot cavity

Observation of reduction of radiation-pressure-induced rotational anti-spring effect on a 23 mg mirror in a Fabry–Perot cavity

Yutaro Enomoto[1], Koji Nagano[1], Masayuki Nakano[1], Akira Furusawa[2] and Seiji Kawamura[1]

[1] Institute for Cosmic Ray Research, The University of Tokyo, Kashiwa, Chiba 277-8582, Japan
[2] Graduate School of Engineering, The University of Tokyo, Bunkyo, Tokyo 113-0033, Japan

E-mail: yenomoto@icrr.u-tokyo.ac.jp

Abstract

Although quantum radiation pressure noise could limit the sensitivity of the second-generation gravitational wave detectors, it has not been observed in a broad frequency band and its reduction methods have not been proven yet. A promising way to observe quantum radiation pressure noise is to store high power light in an optical cavity with a tiny mirror. However, anti-spring torque caused by radiation pressure of the light acting on the tiny mirror could make the system unstable, and it is generally difficult to attach actuators to the tiny mirror for stabilization. Hence a new method to overcome this anti-spring torque has been developed. In the new method, the other mirror of the cavity is controlled so that the position of the resonant light at the tiny mirror is fixed to decrease the anti-spring torque and stabilize angular motion of the tiny mirror. With the new method, it was successfully observed that the anti-spring torque caused by radiation pressure was suppressed in the present experiment with a 23 mg mirror, where resonant frequency of angular motion of the tiny mirror increased towards the mechanical resonant frequency.

Keywords: gravitational waves, interferometry, radiation pressure, Fabry–Perot cavity, anti-spring, feedback

(Some figures may appear in colour only in the online journal)

1. Introduction

The second-generation ground-based laser interferometric gravitational wave detectors, Advanced LIGO in the USA [1], Advanced Virgo in Italy [2] and KAGRA in Japan [3] are expected to achieve their design sensitivities within several years. Quantum noise will be one of the major noise sources in these detectors, especially for KAGRA, where the design sensitivity will be limited by quantum noise in almost all the observation frequency band [3]. Therefore, in order to improve sensitivity of a gravitational wave detector further and develop gravitational wave astronomy, it is necessary to establish methods to reduce quantum noise.

In the case of these detectors, because high power light resonating in cavities (~ 100 kW–l mW) hits mirrors, it is anticipated that radiation pressure noise, which is one of the two kinds of quantum noise, will be the dominant noise source in the low frequency band [1, 2, 4]. For the reduction of radiation pressure noise, a method where the output field of the interferometer is detected with homodyne detection was proposed [5]. In KAGRA, it is planned to use the optical spring effect caused by the radiation pressure of resonant light and the ponderomotive squeezing effect [6, 7] for the reduction of radiation pressure noise [3, 4]. However, radiation pressure noise has never been observed in a broad frequency band and techniques for its reduction have not been proven experimentally. Therefore, it is crucial to construct and confirm the techniques before they are used for the large detectors. To experimentally confirm the techniques, it was proposed to use high-finesse cavities with a milligram scale mirror as arm cavities of a Fabry–Perot Michelson interferometer and store high power resonant light in the cavities [8]. This experimental method is effective in the sense that radiation pressure noise is intentionally made prominent and therefore the experimental system is specialized for the purpose of observation of radiation pressure noise and its reduction; the Michelson interferometer separates the output light from classical noise of the incident light, and a milligram scale mirror and high power light enlarge the displacement caused by radiation pressure of resonant light in the cavity.

In order to realize this experimental method, it is crucial to stably control cavities against high radiation pressure acting on the mirrors of the cavities due to high intra-cavity power of the resonant light. One of the major problems that has to be overcome to realize stable control on the cavities is that the radiation pressure causes anti-spring torque on the mirrors (Sidles–Sigg effect) [9, 10] and then angular motion of the mirrors will be unstable when the anti-spring torque exceeds mechanical restoring torque on the mirrors caused by suspension wires of mirrors. In fact, if actuators are attached to the mirrors for the control of the angular motion of the mirrors, this instability can be avoided [11]. Unfortunately, however, because a milligram scale mirror is so small that it is difficult to attach actuators to it, this problem, potential instability of the angular motion of a mirror, turns out to be serious in experiments with a tiny mirror. The effect of this problem was observed as a decrease of resonant frequency of angular motion of a tiny mirror [12]. The situation is similar for any experiments with cavities that have mirrors with no actuators, and that are susceptible to radiation pressure. We have therefore developed and tested a new method to overcome this problem.

2. Theory

The mechanism of the Sidles–Sigg effect is explained in figure 1. When the right mirror rotates clockwise, the center of curvature of the right mirror shifts upwards and then the resonant axis of the cavity changes. Since the change of the axis is calculated geometrically, the displacement of the position of the resonant light in the cavity (the beam spot) at the right
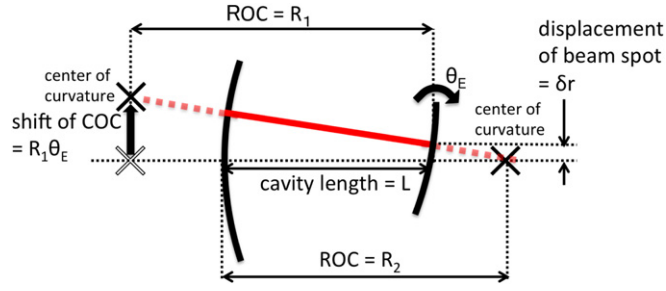
Figure 1. Schematic picture of how the resonant axis of a cavity changes when a mirror of the cavity rotates. θ_E represents rotation angle of the right mirror, R_1 is radius of curvature (ROC) of the right mirror, R_2 is that of the left mirror and L is the length of the cavity. δr denotes the displacement of the beam spot at the right mirror. The solid line and the dotted lines represent path of the resonant light and its extensions, respectively.

mirror is also calculated as

$$\delta r = \frac{R_1 (R_2 - L)}{R_1 + R_2 - L} \, \theta_E. \tag{1}$$

The displacement of the beam spot at the right mirror determines the point at which radiation pressure force acts on the mirror, and therefore causes torque on the mirror so that the expression of the torque on the mirror caused by the radiation pressure of the resonant light T_{RP} is

$$T_{RP} = F_{RP} \frac{R_1 (R_2 - L)}{R_1 + R_2 - L} \, \theta_E. \tag{2}$$

Here F_{RP} is the force caused by radiation pressure of resonant light in the cavity, which follows the relation $F_{RP} = \frac{2P}{c}$, where c is the speed of light and P is the intra-cavity power of the light. The torque can also be expressed in terms of g-factors

$$g_i = 1 - \frac{L}{R_i} \qquad (i = 1, 2), \tag{3}$$

as follows:

$$T_{RP} = F_{RP} \frac{L g_2}{1 - g_1 g_2} \, \theta_E. \tag{4}$$

If $R_2 > L$, $F_{RP} L g_2 / (1 - g_1 g_2)$ is positive so that the torque serves as an anti-spring to the right mirror. In our experimental system, the right mirror is flat, i.e. $R_1 = \infty$, which means that an inequality $g_1 > 0$ always holds and therefore another inequality $R_2 > L$ also always holds due to the resonant condition of a cavity, $0 < g_1 g_2 < 1$ [13].

The above explanation for the Sidles–Sigg effect indicates that if the beam spot position at a mirror is fixed at a certain point the anti-spring effect on the mirror does not occur. Therefore, a control system that suppresses the displacement of the beam spot on the right mirror by feeding back the displacement to the angle of the left mirror, which is described schematically in figure 2, works to reduce the anti-spring effect.

A block diagram of the present control system is shown in figure 3. From here for simplicity, let us restrict ourselves to the case that the right mirror is flat, i.e. $R_1 = \infty$, and let us rename $R_2 \equiv R$. When the rotation of the left mirror is considered, equations (1) and (2)
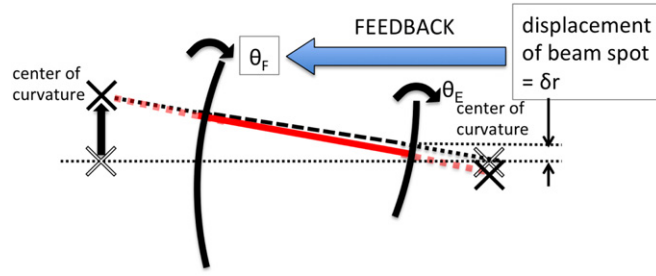
Figure 2. Schematic picture of the present control method. Torque is applied on the left mirror according to measured δr. The thick solid line and the thin dashed line represent the light paths of the resonant light with and without the torque applied on the left mirror, respectively.
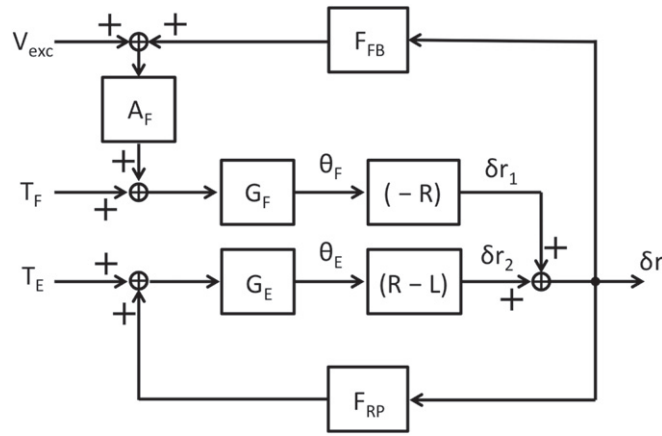

Figure 3. Block diagram that describes rotational motion of the system. $T_{F(E)}$ is external torque acting on the left (right) mirror. $G_{F(E)}$ is angular susceptibility of the left (right) mirror. R is radius of curvature of the left mirror. L is the cavity length. F_{RP} is force caused by radiation pressure of the resonant light in the cavity. F_{FB} corresponds to the transfer function of the feedback filter. V_{exc} is excitation voltage signal that can be added into the upper feedback loop. A_F is efficiency of the actuator attached to the left mirror.

are generalized as

$$\delta r = \delta r_2 + \delta r_1 = (R - L)\theta_E - R\theta_F, \tag{5}$$

$$T_{RP} = F_{RP}[(R - L)\theta_E - R\theta_F], \tag{6}$$

respectively. Since the transfer function from δr_2 to δr is $1/(1 + H)$ according to the block diagram, the expression of anti-spring torque acting on the right mirror turns out to be

$$T_{RP} = \frac{1}{1 + H}F_{RP}(R - L)\theta_E, \tag{7}$$

where $H = F_{FB}A_F G_F R$. This formula shows that the anti-spring torque T_{RP} is suppressed by $1 + H$, and it is possible to reduce the anti-spring effect on the mirror by exploiting the freedom of chosing F_{FB} [14]. To understand the meaning of equation (7), let us consider the
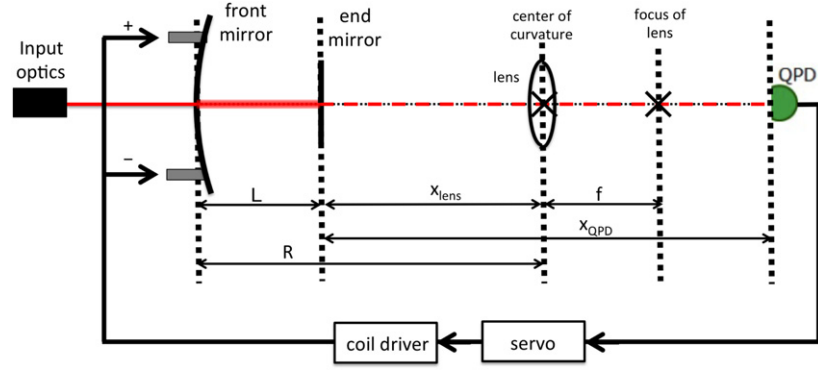
Figure 4. Schematic diagram of the experiment. The laser light injected from the input optics resonates in the cavity. The transmitted light of the cavity is measured with a quadrant photodetector (QPD). The output of the QPD is fed back to the actuators attached to the front mirror.

case that $|H| \gg 1$ as an example. $|H| \gg 1$ means that the gain of the upper feedback loop in figure 3 is so high that $\delta r \simeq 0$ and the torque caused by radiation pressure no longer acts on the right mirror. In terms of the block diagram, since $1/(1 + H)$ can be regarded as 0, the lower feedback loop of the anti-spring torque in figure 3 can be neglected.

Although a solid way to observe the reduction of the anti-spring effect on the right mirror is to measure the susceptibility θ_E/T_E directly, it is not easy to measure θ_E/T_E if the mirror has no actuators; it is not possible to apply torque directly to the mirror. We developed a method to obtain the susceptibility by exciting the mirror motion with radiation pressure of the resonant light of the cavity itself and measuring the transfer function $\delta r/T_F$ in the case that $F_{FB} = 0$ [15]. It is beneficial to measure δr instead of θ_E to obtain the susceptibility because external torque on the right mirror T_E will affect the measurement less. In application of this method, it is possible to measure the susceptibility in the case that $F_{FB} \neq 0$ in the following way. The transfer function $\delta r/T_F$ is expressed as

$$\frac{\delta r}{T_F} = \frac{-\frac{G_F R}{1 + H} G_E^{-1}}{G_E^{-1} - \frac{1}{1 + H} F_{RP}(R - L)}. \tag{8}$$

Once this function is measured, the angular susceptibility of the right mirror is calculated as

$$\frac{\theta_E}{T_E} = \frac{G_E}{1 - \frac{1}{1 + H} G_E (R - L) F_{RP}} \tag{9}$$

$$= -\frac{\delta r}{T_F} \frac{1 + H}{G_F R} G_E. \tag{10}$$

If H, G_F and G_E are known, equation (10) shows that the susceptibility is obtained by measuring $\delta r/T_F$. In fact, H, G_F and G_E are measurable with auxiliary experiments. Note that $\theta_E/T_E \to G_E$ when $|H| \to \infty$. This behavior is consistent with the interpretation of equation (7) that the anti-spring torque no longer acts on the right mirror with large $|H|$.
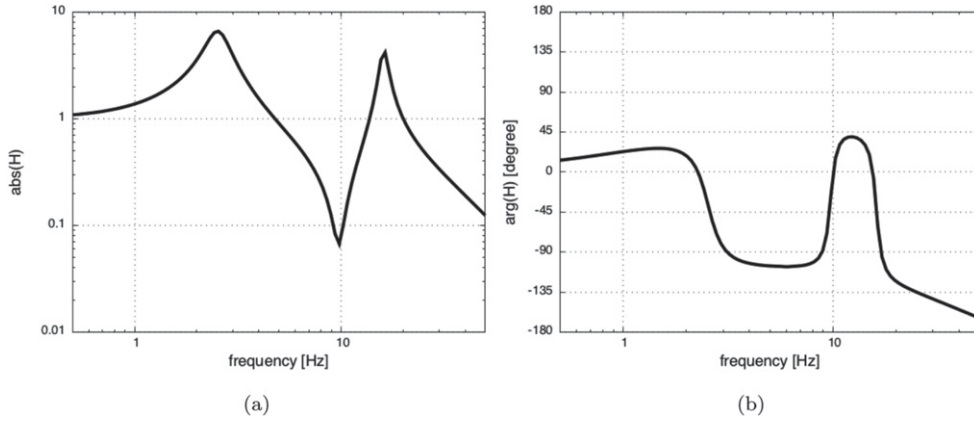
Figure 5. Open loop transfer function of the upper loop of the block diagram shown in figure 3: $H = F_{FB}A_F G_F R$. Overall gain constant was variable. In this figure, the gain constant is set for the gain at DC to be unity. These traces were obtained by fitting measured data with the theoretical curve of H.

3. Experiment

The setup of our experiment is schematically described in figure 4. The light source we used is a Nd:YAG laser of wavelength 1064 nm. The power of the light injected into the cavity was about 35 mW. The length of the cavity is 14 cm. The finesse of the cavity was about 600. The radius of curvature of the front mirror is 1 m, its diameter is 25.4 mm, and its mass is 55 g. It is suspended in double pendulum structure, and four magnets are attached to it so that its translational, yaw, and pitch degrees of freedom can be actuated independently through four coils that are located behind the front mirror. The end mirror is a tiny mirror made of fused silica whose mass is 23 mg. It is flat and its diameter is 3 mm. It is suspended by a silica fiber of 10 μm in diameter from the intermediate mass that is suspended by a tungsten wire from a metal structure fixed to the breadboard. The breadboard supports both mirrors of the cavity. The cavity length was controlled with the actuator attached to the front mirror using Pound–Drever–Hall method [16] so that the cavity was kept resonant. A quadrant photodetector (QPD) and a lens were placed in such a way that the beam spot position at the QPD is exactly the same as that at the end mirror. This condition is realized explicitly by the parameter set of $x_{lens} = R - L$, $x_{QPD} = 2(R - L)$, $f = (R - L)/2$. Therefore we adopted $x_{lens} = 0.86$ m, $x_{QPD} = 1.7$ m, and $f = 0.4$ m.

Mechanical characteristics of the yaw motion of the mirrors had been measured [15]. If it is assumed that the yaw motion of the end mirror is described as a single oscillator, i.e.

$$G_E(f) = \frac{1}{4\pi^2 I} \frac{1}{f_0^2 + if_0 f/Q - f^2}, \tag{11}$$

the moment of inertia about the axis passing through the diameter I is 1.7×10^{-11} kg m^2, the resonant frequency f_0 is 2.62 Hz, and the Q-value is 6.7. The susceptibility of the front mirror is described well with a coupled oscillator model in which resonant frequency and Q-value for the lower frequency mode are 2.54 Hz and 3.76, respectively, and resonant frequency and Q-value for the higher frequency mode are 15.9 Hz and 21.4, respectively.

The open loop transfer function of the upper loop in figure 3, H, was obtained as shown in figure 5. The efficiency of the actuator is assumed to be constant with respect to frequency.
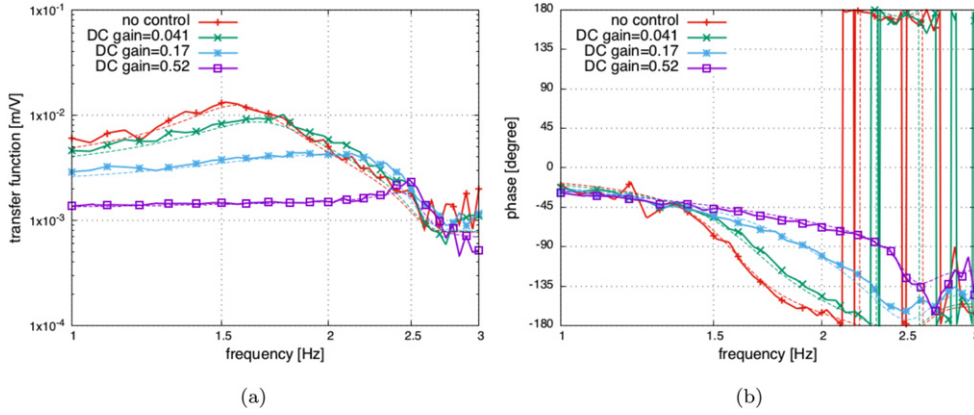
Figure 6. Transfer functions $\delta r/V_{\mathrm{exc}}$. Although the transfer functions were measured for eight values of the gain at DC, $H(f=0)$, only four are shown as representative for clarity. Thick lines with markers correspond to measured data and thin dashed lines correspond to theoretical curves with $H(f=0)$ translated from measured $F_{\mathrm{FB}}(f=0)$.

The filter circuit was designed so that its transfer function ensured the stability of the upper loop. The circuit contains a variable gain amplifier (VGA). By measuring $\delta r/V_{\mathrm{exc}}$ ($\propto \delta r/T_{\mathrm{F}}$) for several values of gain of VGA, we observed how the susceptibility of the end mirror changed in accordance with the change of the gain of the loop.

4. Results

The transfer functions $\delta r/V_{\mathrm{exc}}$ were measured as shown in figure 6. The intra-cavity power of the resonant light was expected to be 5.1×10^2 mW. This value of the intra-cavity power was consistent with the previous result [15]. Measured transfer functions $\delta r/V_{\mathrm{exc}}$ were explained well with theoretical curves as shown in figure 6, with $H(f=0)$, the gain of the upper loop in the block diagram in figure 3 at DC, calibrated as described in the next paragraph.

The gain $H(f=0)$ for each measurement was calibrated as follows: each $\delta r/V_{\mathrm{exc}}$ was fitted by theoretical curve using $H(f=0)$ as a single fitting parameter and maximally likely estimation of $H(f=0)$ was assigned for each, measured values of $F_{\mathrm{FB}}(f=0)$ were assumed to be proportional to the assigned values of $H(f=0)$, and measured values of $F_{\mathrm{FB}}(f=0)$ were translated into $H(f=0)$ using the obtained constant of proportionality between F_{FB} and H.

Each susceptibility of the yaw motion of the tiny mirror obtained by converting $\delta r/V_{\mathrm{exc}}$ into $\theta_{\mathrm{E}}/T_{\mathrm{E}}$ with equation (10) is shown in figure 7. Figure 7 shows that the peak frequency of the susceptibility shifted higher and the susceptibility approached the mechanical susceptibility G_{E} when the gain, $H(f=0)$, was set larger, as equation (7) indicates. Each susceptibility $\theta_{\mathrm{E}}/T_{\mathrm{E}}$ obtained from measurement matched well with one obtained theoretically, as shown in figure 7. In other words, figure 7 quantitatively describes the coincidence between measured and theoretical shifts of the resonant frequency. Here since the relation $|H| \gg 1$ did not hold, the susceptibility did not completely approach the mechanical susceptibility G_{E}. This result shows that the feedback control from δr to T_{F} prevents the resonant frequency of the angular motion of the tiny mirror from decreasing. The measurement
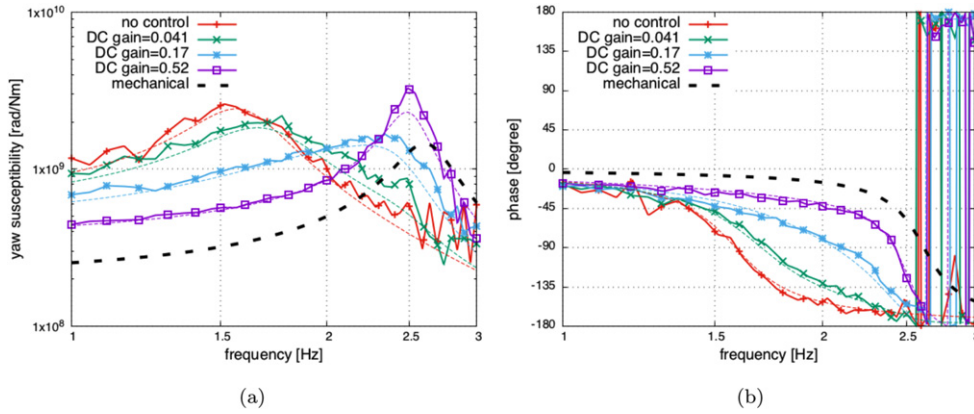
Figure 7. Obtained susceptibilities of the yaw motion of the tiny mirror, θ_E/T_E. Although the susceptibilities were obtained for eight values of the gain at DC, $H(f=0)$, only four susceptibilities are shown as representative for clarity. Thick lines with markers correspond to measured data, thin dashed lines correspond to theoretical curves, and a bold dashed line is the mechanical transfer function, G_E.

therefore demonstrates that the anti-spring effect on the mirror is reduced when the gain of the present control loop increases.

5. Conclusion and discussion

The present result successfully proves for the first time that the Sidles–Sigg instability on a tiny mirror with no actuators can be reduced by the feedback control from the beam spot position at the mirror to angular motion of the other mirror of the cavity. Therefore, the demonstrated control method is proven to be useful for the stable control of an optical cavity with a tiny mirror against high intra-cavity power of the resonant light, which is crucial for observation and reduction of quantum radiation pressure noise.

Let us discuss the effect of this control method on misalignment of the cavity in figure 2. Figure 2 shows that if the right mirror rotates, this control rotates the left mirror and shifts the beam spot towards the center of the left mirror. Thus, this control method reduces the displacement of the beam spot from the center of both mirrors. Moreover, the rotation of the left mirror caused by external disturbances is suppressed by this control method, because externally induced rotation of the left mirror causes the displacement of the beam spot position at the right mirror, which is detected and fed back to the rotation of the left mirror in this control method. In fact, it can be shown that the above two discussions hold for resonant cavities with any geometry. Therefore, besides the reduction of the torque on the right mirror caused by radiation pressure of the resonant light, this control method effectively improves alignment of the cavity against external sources of rotation.

This result is potentially applicable to any experiments that employ a cavity with a tiny mirror which actuators cannot be attached to, such as ground state cooling experiments [17] and optical levitation experiments [18].

Acknowledgments

References

[1] Aasi J *et al* 2015 Advanced LIGO *Class. Quantum Grav.* **32** 074001
[2] Acernese F *et al* 2015 Advanced virgo: a second-generation interferometric gravitational wave detector *Class. Quantum Grav.* **32** 024001
[3] Aso Y, Michimura Y, Somiya K, Ando M, Miyakawa O, Sekiguchi T, Tatsumi D and Yamamoto H 2013 Interferometer design of the KAGRA gravitational wave detector *Phys. Rev.* D **88** 043007
[4] Somiya K 2012 Detector configuration of KAGRA-the Japanese cryogenic gravitational-wave detector *Class. Quantum Grav.* **29** 124007
[5] Kimble H J, Levin Y, Matsko A B, Thorne K S and Vyatchanin S P 2001 Conversion of conventional gravitational-wave interferometers into quantum nondemolition interferometers by modifying their input and/or output optics *Phys. Rev.* D **65** 022002
[6] Buonanno A and Chen Y 2001 Quantum noise in second generation, signal-recycled laser interferometric gravitational-wave detectors *Phys. Rev.* D **64** 042006
[7] Buonanno A and Chen Y 2002 Signal recycled laser-interferometer gravitational-wave detectors as optical springs *Phys. Rev.* D **65** 042001
[8] Sakata S 2008 Study of the reduction of the radiation pressure noise in gravitational wave detectors using the ponderomotive squeezing *PhD Thesis* Ochanomizu University
[9] Sidles J and Sigg D 2006 Optical torques in suspended Fabry–Perot interferometers *Phys. Lett.* A **354** 167–72
[10] Solimeno S, Barone F, Lisio C D, Fiore L D, Milano L and Russo G 1991 Fabry–Pérot resonators with oscillating mirrors *Phys. Rev.* A **43** 6227–40
[11] Dooley K L, Barsotti L, Adhikari R X, Evans M, Fricke T T, Fritschel P, Frolov V, Kawabe K and Smith-Lefebvre N 2013 Angular control of optical cavities in a radiation-pressure-dominated regime: the enhanced LIGO case *J. Opt. Soc. Am.* A **30** 2618–26
[12] Sakata S, Miyakawa O, Nishizawa A, Ishizaki H and Kawamura S 2010 Measurement of angular antispring effect in optical cavity by radiation pressure *Phys. Rev.* D **81** 064023
[13] Kogelnik H and Li T 1966 Laser beams and resonators *Appl. Opt.* **5** 1550–67
[14] Nakano M 2014 Study of opt-mechanical cavity control for development of quantum noise reduction in KAGRA gravitational wave detector *Master's Thesis* University of Tokyo
[15] Nagano K, Enomoto Y, Nakano M, Furusawa A and Kawamura S 2016 New method to measure the angular antispring effect in a Fabry–Perot cavity with remote excitation using radiation pressure *Phys. Lett.* A **380** 983–8
[16] Drever R W P, Hall J L, Kowalski F V, Hough J, Ford G M, Munley A J and Ward H 1983 Laser phase and frequency stabilization using an optical resonator *Appl. Phys.* B **31** 97–105
[17] Genes C, Vitali D, Tombesi P, Gigan S and Aspelmeyer M 2008 Ground-state cooling of a micromechanical oscillator: comparing cold damping and cavity-assisted cooling schemes *Phys. Rev.* A **77** 1–9
[18] Guccione G, Hosseini M, Adlong S, Johnsson M T, Hope J, Buchler B C and Lam P K 2013 Scattering-free optical levitation of a cavity mirror *Phys. Rev. Lett.* **111** 183001